140 KSME Journal, Vol. 2, No. 2, pp. 140~146, 1988.

NOISE CONTROLS IN THE TURBULENCE MEASUREMENTS THROUGH THE CONTRACTION BY THE SPECTRAL TECHNIQUES

Yong Oun Han*

(*Received October 22, 1988*)

In the grid turbulence measurements through a contraction, the background noises are classified into two distinct groups; electrical noises and flow contaminations, and the latter were rather out of controls once they appear in the measurements. It was found that the flow contaminations are amplified as the rate of flow contraction along the channel, and that these cause the additional reading of the longitudinal turbulence to the hot wire sensor, especially. Using the pure grid effect turbulence, obtained by the subtraction method and the spectrum measurments, the readings of longitudinal turbulence were reduced substantially with a maximum of 1.5%, comparing to those which were obtained in the traditional way. This additional reading was suspected to cause a critical effect in analyzing the turbulence energy transition through the contraction flow, in which the turbulence intensity was at best 5%, or less.

Key Words: Pure Grid Turbulence, Subtraction Hypothesis, Upstream Flow Contamination, Derivative Spectrum, Contraction Turbulence

NOMENCLATURES

e_i : Input voltage signal in first order system
e_o : Output voltage signal in first order system
f : Frequency
f_{HP} : High pass filtering frequeccy
i : $\sqrt{-1}$
L : Pipe length
N : Number of independent realizations
n : Integer for n-th harmonic
$S(f)$, S_u : Velocity spectrum
$S_{\dot{u}}(f)$: Derivative spectrum
$S(0)$: Half line spectrum at zero frequency
T : Record length
t, t' : Time
$\boldsymbol{u}$: Mean velocity
u : Longitudinal turbulence
$\overline{u^2}$: Longitudinal turbulence square mean
$\overline{\dot{u}(t)\,\dot{u}(t+t')}$: Correlation of longitudinal derivative turbulence
η : Kolmogoroff microscale
τ : Time integral scale

Subscripts

g : Gird
k : Kolmogoroff
ng : Nongrid
o : Pure value(subtracted)

*Department of Precision Mechanical Engineering, Yeungnam University, Gyongsan 713-749, Korea

1. INTRODUCTION

The contraction flow develops the vortex stretching mechanism downstream so that the lateral turbulence becomes larger and the longitudinal one smaller than those of upstream. The usual order of the magnitude of turbulence intensity in internal flows is known to be less than 5% of the mean velocity. Therefore, in the contraction flow with the area ratio of 1 : 10.5, it is expected to be less than 0.5% of the turbulence intensity near the smallest area section when it is normalized by the local mean velocity variation. In this flow, even slight upstream flow contaminations may cause critical effect on the downstream turbulence measurements. Therefore, a detail analysis about the upstream flow conditions must be preceded before taking any measurement. In most measurements through flow channels, two different kinds of noises are detected; one is the electrical noise, the other is the flow source contamination from the mechanical and the acoustical disturbances in the upstream. The original flow source contamination from the flow generating units is rather out of control once they appear, while the electrical noises from wirings, instruments and electrical equipments in laboratory have been overcome by high signal-to-noise ratio using gainers and filters mostly. Therefore, a careful design and fabrication of the flow generating device is the only way to avoid these ill conditions. However, fortunately, the flow contamination can be distinguished from the electrical noises through the contraction device because it is amplified as the contraction ratio while the electrical noises stay at the same level as those of upstream. Therefore, there is a possibility to reduce the flow contamination in a certain way, say, a subtraction which will be described in detail later.

In the other aspect, the contraction has been considered as an essential device for accelerating the flow, for example, in

a wind tunnel design, locating at just before the test section, and in a nozzle design, being as a flow terminating device. But, for computational turbulence modellers, it has been dealt with as a favorite device to make turbulence highly anisotropy to understand the so called 'return-to-isotropy' (Lumley and Neuman, 1977: Comte-Bellot and Corrsin, 1966).

In previous measurements such as Uberoi(1956) and Ramjee et al(1976), the negative dissipations were detected in turbulence energy balance which were calculated from the difference between the production term and the mean convection term, ignoring the turbulence transport term, which was done in Shabbir(1983). Such physical unreality seemed to be due to the upstream contamination which increased the longitudinal turbulence more than the lateral(Han, 1988). Therefore, removal of the upstream contamination is essential to secure the physical realizability. Through this work it will be shown that the subtraction technique is the prospective way to get rid of the upstream contamination when a proper statistical criterion is provided. In order to carry out this work, a grid generated turbulence was used as a turbulence source and a pure grid generated turbulence was obtained by the subtraction technique.

2. EXPERIMENTAL CONDITIONS

2.1 Experimental Facilities and Instruments

The experiments were carried out by using an experimental facility which consists of five main units; a blower, a flow conditioning unit which was made with three screens and two honeycombs, a grid, a straight duct which has the same circular section as that of the contraction inlet, and a contraction. The actual turbulence generator was the biplane grid constructed with circular steel rods of 0.25 inch diameter. The rods were assembled to have one inch square mesh and the 40% of solidity. The grid was positioned 24 in ahead of the contraction inlet in the straight circular duct whose diameter was 19.5 inches so that the homogeneity of grid turbulence, which is usually established 40 times grid mesh lengths downstream from the grid section, will appear around the exit of contraction if the flow not contracted(Corrsin, 1963). The contraction was of matched cubic design with the matching point at 50% of the distance in the direction from the entrance to exit and has the area ratio of 1 : 10.5, which yields the following mean velocity distribution along the centerline(Fig. 1).

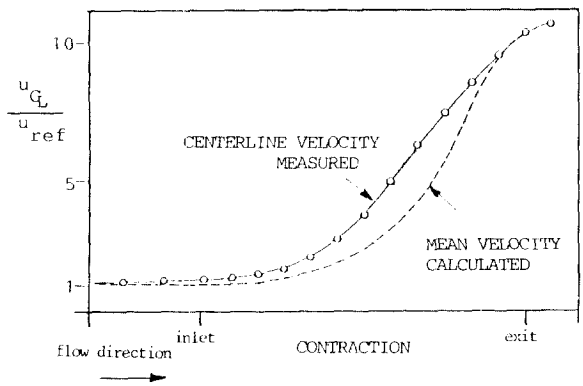

Fig. 1 Centerline velocity measured and mean velocity calculated based on the continuity

Flow velocities were measured by the hot-wires, based on the CTA system, Dantec 55M01, with 55M10 bridges. The hot-wires were of single and X-wire configurations and were constructed from 5 micron meter diameter copper-plated tungsten wire welded onto Dantec 55P01, 55P51 probe bodies, respectively. The wire length was approximately 3 mm of which the active portion(etched length) was the center of 1.2 mm long, which gives the effective length-to-diameter ratio of 240. The anemometers were usually operated at the highest possible gain settings consistent with their stability(Gain=6) and on overheat ratio of 0.6 which was consistent with minimizing the sensitivity to the slight fluctuations in temperature in the room and maximizing probe life.

Because of the relatively weak turbulence intensity in the flow(typically 1% or less) and the corresponding low rms voltages associated with the anemometer signal(typically 0.5%), it was desirable to amplify the AC part of the signal in order to utilize the widest possible range of the A/D converter, thereby, minimizing the quantization noise. This was accomplished by passing the anemometer signals through the Dantec 55D26 signal conditioning units which contain both adjustable high-and low-pass filters(at both 6 and 18 dB/Octave) and amplifiers. The low-pass filter cutoff frequency ranges from 200 Hz to 1.3 kHz depending on the position through the contraction and the roll-offs, at −18 dB/Octave to provide an anti-aliasing filter.

In order to investigate what kind of disturbances were introduced into the flow from the blower, an accelerometer, KISTLER Model 8628A5, which has the measurable range in frequency between 1 Hz and 2 MHz, and a dual mode amplifier, KISTLER Model 5004 were used. The amplified analog outputs from the accelerometer and the hot-wires were processed with a dual channel FFT spectrum analyzer(Nicholet Scientific Co. Model 660A) and an interactive digital plotter(TEKTRONIX Model 4662) for observing the coherence between their amplified signals.

The calibration of the hot-wires was followed by the digital linearizing scheme detailed by George et al(1987) in which the cooling velocity is calculated as a power series of the anemometer output voltage. The angle calibration of X-wire was carried out with a modified cosine law worked done by Champagne & Sleicher(1967) and the k-factors were 0.02 and 0.025 for both wires respectively at the constant chamber velocity of 2m/sec.

2.2 Data Acquisition and Processing

The signals from the two anemometers of X-wire were first passed through the signal conditioners which amplified the fluctuating parts of the signal and removed the DC parts (below 1 Hz). These two signals were later used for calculating the fluctuating parts of the turbulence only. In order to obtain mean velocities, the outputs from the same anemometers were separately fed through the anti-aliasing filters which were Bessel low-pass active filters(Frequency Devices Model 848p81-5). The signals were digitized using a 16 bit A/D converter with the maximum throughput rate of 150 kHz, a quantization error less than 0.01%. The A/D converter was interfaced with a DEC PDP 11/84 minicomputer using the DEC DRll-W interface module. A DEC RA81 500 mega byte disk drive and the DEC TU81 high speed tape driver were used for storage of the data. An on-site Microvax and remote Vax-cluster were used for data processing.

In order to get a proper sampling criterion for the moment measurements, the integral time scales were measured along

the centerline of the contraction in every one inch to calculate the record length T for the convergence. The effective number of independent realizations N, was obtained by the relation; $N=T/2\tau$ and the integral scale $\tau=S(0)/4\bar{u}^2$, where $S(0)$ is a half line spectrum measured by the analog spectrum analyzer. As a result, the largest integral time scale was around 0.1 second near the entrance of the contraction for the axial component. The radial ones were assumed to be similar to the axial one(Uberoi, 1956). In these measurements a 0.125 second was used for carrying out moment measurements with safety, as the largest integral time scale τ_{max}. In order to minimize both quantities of data and acquisition time, 1024 samples were taken at the optimal rate of $1/2\tau_{max}$ or, approximately 4 Hz, which corresponds to the record length of 250 sec. This assured the variability with respect to the mean to be within 0.4%, when they are ensemble-averaged(George, Beuther and Lumley, 1978).

For the spectral measurements, the sampling frequency were calculated from $f_K=U/2\pi\eta$, where the Kolmogoroff microscale η is given by$(\nu^3/\varepsilon)^{1/4}$. The dissipation ε was estimated from the turbulence kinetic energy equation. Near the chamber, f_k was found to be about 250 Hz at 2m/sec of mean velocity. Therefore, 2.5 kHz was chosen as the initial guess because the mean velocity in the contraction is about ten times of the chamber velocity. Finally, a sampling rate of the 5 kHz was selected with the safe factor 2. Actually, in the preliminary trials, most energy of the spectra had been found to be within 500 Hz, which proves the validity about the initial guesses. The spectra were ensemble-averaged over 99 blocks(each block has 1024 data points) so that the variability for each spectral value was about 14% based on the works of George et al(1978).

3. NOISE ANALYSES

3.1 Overview of Noises Detected

Although the origins of noises detected in these measurements were not unveiled completely, the following noises were measured and analyzed with typical instruments as mentioned before; a weak vibration of the blower motor casing at 25 Hz which was small enough not to be detectable on other general case except the contraction flow measurement, the straws' acoustic effects of honeycomb at around 400 Hz and its harmonics, the blade passing frequency at 220 Hz,

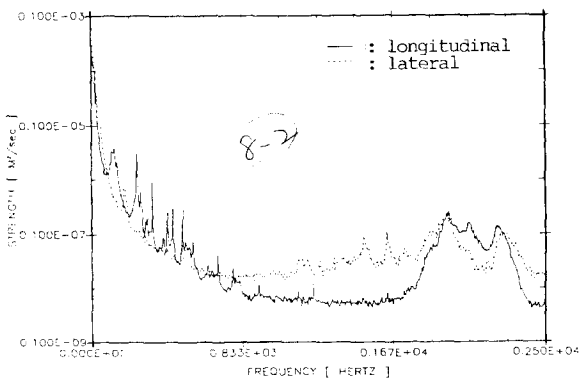

Fig. 2 Raw hot-wire velocity spectra at inlet of contraction before noise reductions

a wind tunnel body organ effect at 17, 54, 85 Hz,..., an air breeding gab acoustics in the stabilizing unit around 500 Hz, the high frequency aliasing contamination at 170, 300, 650 Hz. s the instrument interferances from the anntena effects at 2 kHz around, a typical 60 Hz peak from the poor shielding and grounding in wiring, some peaks from the digital processing units at 3k, 10k Hz.s(seemed to be from the computer) and, of course, many unknown noises as shown in the power spectrum measurements(Fig. 2).

These noises may be classified into two different kinds; one is the noises from the flow source and the flow channel structure including the contraction which will be called 'the upstream flow contamination' from now on, and the other comes from the electrical equipments used for the experiments and the laboratory surroundings. The latter can be reduced by putting the high signal to noise ratio and by setting the proper low-pass filtering for high frequency noises.

3.2 Electrical Noises

The typical AC noise occurred at 60 Hz during the preliminary experiment which comes from the poor shielding and grounding between the coax BNC cord and the connecting jack, mostly. From the hot-wire probe to the reading device, the same level ground was seeked by constructing the parallel outlet power stripe, out of which two anemometers and two signal conditioners could have parallel link without any potential loss. And every reading device was also parallel. The anntena effect was rather critical to the lining about 20 m cables. Every single line was avoided from the crossing and adjacency of other cables. Many of these noises including the 60 Hz were below the amplified ouput level which was gained 100 times through the signal conditioner over the whole experiments. And these amplified data were scaled back through the software during data processing by dividing the same gains.

The unknown high frequency noises were detected at 3 kHz, 10 kHz, around which were seemed to occur always wherever the digitizing processor, computer, A/D converter and active filter sets may be used close to the experimental units. The active aliasing filter set and the low-pass filter of signal conditioner were utilized to get rid of the high frequency noise contaminations by setting the low-pass filter 2. 5 kHz for the mean value, and the low-pass filtering at about 800Hz~2kHz being dependent on the distance through the contraction, for rms value, respectively.

Besides the above noises which can be controlled by the electrical technique, more intrinsic instrumental noises must be reduced by any possible means which are normally composed of the differentiation and integration techniques, or iteration of these in turns, by the analog equipments and softwares. The usage of the resistor and the active filter naturally cause the noise effects in a certain fashion that the resistor mean square noise is proportional to the multiple of room temperature times resistance and the active filter makes the high frequency noise big(Freymuth, 1968). The constant temperature anemometer usually has the feedback loop composed of the bridge and the amplifier which suppresses the thermal lag of the hot-wire, while the constant current anemometer need not to use the bridge. Therefore, the CTA system has the possibility to increase the system noise even though the automatic balancing of the bridge has much more merits, while the CCA can hardly increase the system noise with a simple circuit.

3.3 Upstream Flow Contamination

Flow contamination comes mainly from the mechanical vibrations and the acoustic effects of the flow generating devices and they are usually out of control once they happen. In order to investigate the blower vibration and its effects at downstream, two analog signals, one from the accelerometer on the blower casing and the other from the single wire at contraction exit, were utilized to obtain the coherence between the two. As the results, a peak at 25 Hz around was detected which showed a dynamic unbalance of the blower or, blower casing vibration as one time per revolution, which was inferred from the 80% power operation of blower motor with the maximum rotating speed capability of 1740 rpm (Fig. 3) Several trials such as stiffners on the blower casing, rigid connection by steel bars between the blower and the ground, air breeding gabs, rubber damping pad section of 8″ long, were applied to get rid of that peak but at best they only reduced the peak height. Another inevitable peak in most flow generated by the fan with 9 blades was also appeared at blade passing frequency near 220 Hz around from the hot-wire signal.

The acoustic contaminations were detected at several frequencies in power spectra ; a pipe organ effect of the flow duct including contraction aroung 17, 54, 85 Hz,...even though they were weak, which were based on the equation $(2n\text{-}1)\,c/4L$ for n-th harmonic through the open pipe, where c is the sonic velocity and L is the pipe length (about 5 m here), and the straws' acoustic around 400 Hz based on 0.22 m of straw length in honeycomb. Near the contraction exit, the slight back flow disturbance from the jet entrainment was also suspected in the range less than 300 Hz (Crow and Champagne, 1971). Even though all these flow contaminations were small enough, they will effect the downstream conditions and, as the results, the downstream may have the critical damage in such an internal flow that has the relatively small turbulence intensity (Fig.4).

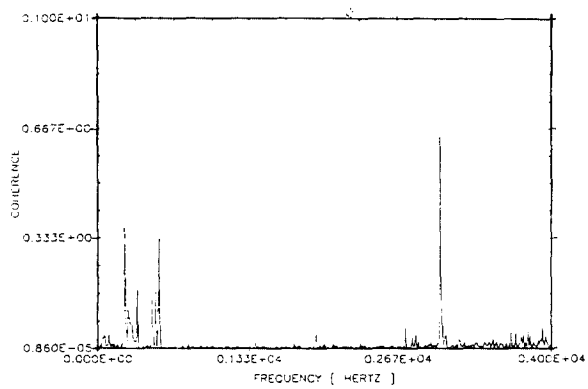

Fig. 3 Coherence between hot-wire at exit of contraction and accelerometer on blower casing

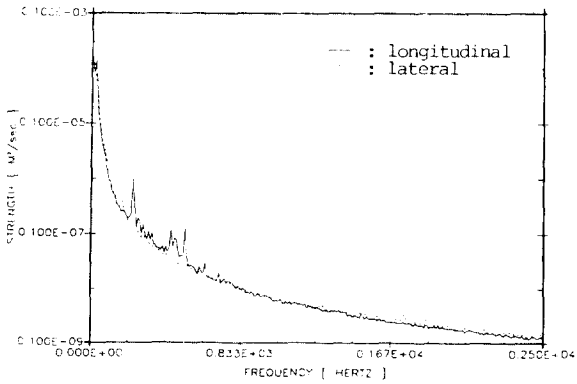

Fig. 4 Raw hot-wire Velocity spectra at inlet of contraction after electric noise reductions

4. IMPROVEMENT OF TURBULENCE

4.1 Subtraction Hypothesis

As the single wire travelled through the contraction the spectra showed that the contamination peaks occured at the same frequencies always and their magnitudes were grown up monotonically to the exit. Therefore, in order to see how the contamination may distribute through the contraction, a parallel wire which was made by two single wires with 2″ separation was applied as the following idea. That is, let $u(t)$ be the contaminated grid turbulence or, the grid turbulence shortly, and $u_o(t)$ a pure grid turbulence which does not include any contamination and $u_n(t)$ a contamination and, then, the output from two single wires which move parallel to the centerline, on the same radial distance, can be split into the following equations, respectively ;

$$\begin{aligned} u_1(t) &= u_{o1}(t) + u_{n1}(t) \quad \text{for wire 1} \\ u_2(t) &= u_{o2}(t) + u_{n2}(t) \quad \text{for wire 2} \end{aligned} \tag{1}$$

And if the flow is axisymmetric and the probes on the same concentric circle and if the flow contamination is uniform at the same section, the relation,

$$u_1(t) - u_2(t) = [u_{o1}(t) - u_{o2}(t)] + [u_{n1}(t) - u_{n2}(t)] \tag{2}$$

will be simplified as the following equation, when two probes read the same noises over the incident section such that $u_{n1}(t) = u_{n2}(t)$

$$u_1(t) - u_2(t) = [u_{o1}(t) - u_{o2}(t)] \tag{3}$$

Therefore, the root mean square of the above equation can be

$$\overline{(u_1 - u_2)^2} = \overline{u_{o1}^2} + \overline{u_{o2}^2} - 2\overline{u_{o1}\ u_{o2}} \tag{4}$$

where $u_1 = u_1(t)$ and $u_2 = u_2(t)$ and from now on, the time variable will be omitted. If a big enough separation is provided so that the pure grid turbulences from two wires might be spatially independent--could be several times of the integral scale, the above equation will be

$$\overline{(u_1 - u_2)^2} = 2\overline{u_o^2} \tag{5}$$

with the correlation $\overline{u_{o1}\ u_{o2}} = 0$ and $\overline{u_{o1}^2} = \overline{u_{o2}^2} \equiv \overline{u_o^2}$ And from the same idea, the equation

$$\begin{aligned} \overline{(u_1 + u_2)^2} &= \overline{(u_{o1} + u_{o2})^2} + \overline{(u_{n1} + u_{n2})^2} \\ &= 2\overline{u_o^2} + 4\overline{u_n^2} \end{aligned} \tag{6}$$

is also possible. Therefore, from the equations (5), (6), the contamination quantities can be traced out by the relation ;

$$\frac{1}{4}\left[\overline{(u_1 + u_2)^2} - \overline{(u_1 - u_2)^2}\right] = \overline{u_n^2} \tag{7}$$

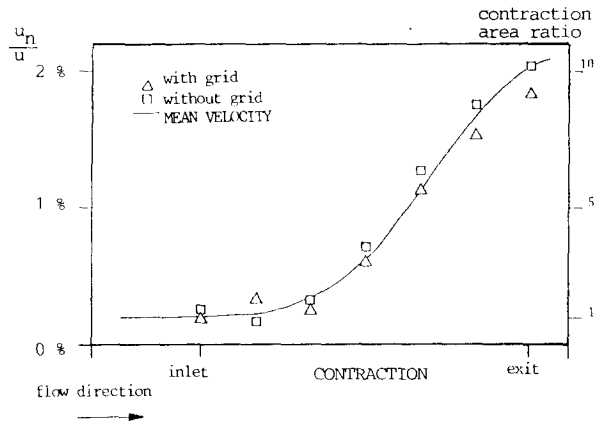

Fig. 5 Variation of contamination levels through contraction calculated for the cases of grid flow and nongrid flow, respectively

theoretically. If this quantity $\overline{u_n^2}$ is the true contamination, it must be grown up at the rate of the mean velocity increase following the continuity, instead of following the vortex stretching mechanism like as the pure grid turbulence does. Therefore, it is desirable to use only the pure grid turbulence in order to look the true turbulence energy transition through the contraction because the grid turbulence also accompanies the upstream contamination before the grid already. By using the same idea, the flow contamination of the nongrid flow were also measured by putting $\overline{u_0^2}=0$ in both equations(5), (6). As the result of both measurements the contaminations calculated for both cases are distributed almost same as the mean velocity profile(Fig. 5).

Therefore, because both cases have almost the same amount of contaminations and the same trends, the pure grid effect turbulence can be obtained by a simple subtraction of the nongrid flow measurement data from those of the grid flow measurement obeying the similar relation;

$$\overline{u_t^2}=\overline{(u_t+u_n)^2}-\overline{u_{ng}^2} \tag{8}$$

with the assumptions of $\overline{u_n^2}=\overline{u_{ng}^2}$ and the correlation $\overline{u_t u_n}=0$, apparently, where u is the true grid effect turbulence, u_n the upstream flow contamination and u_{ng}, the nongrid turbulence which was obtained from the same experiment without the grid section. Of course, the manipulations have to be done after the reduction of the electrical noises.

4.2 Spectral Measurements

The electrically filtered spectra of the grid and the nongrid turbulences respectively, were measured by use of the fast Fourier transform algorithm and plotted in the figures[Figs. 6 (a), (b), (c)]. In most figures of spectra the energies were concentrated within 300 Hz so that the various sampling rate of 800 Hz~1.3 kHz through contraction was safe enough to avoid the aliasing effect based on the Nyquist criteria. The spectrum of the grid generated flow was subtracted by that of the nongrid flow, file-to-file, directly. Each file contains 1024 data in order to match the power of 2 for FFT algorithm.

$$S_g(f)-S_{ng}(f)=S_o(f) \tag{9}$$

where S_g is the spectrum of the grid turbulence, S_{ng}, that of

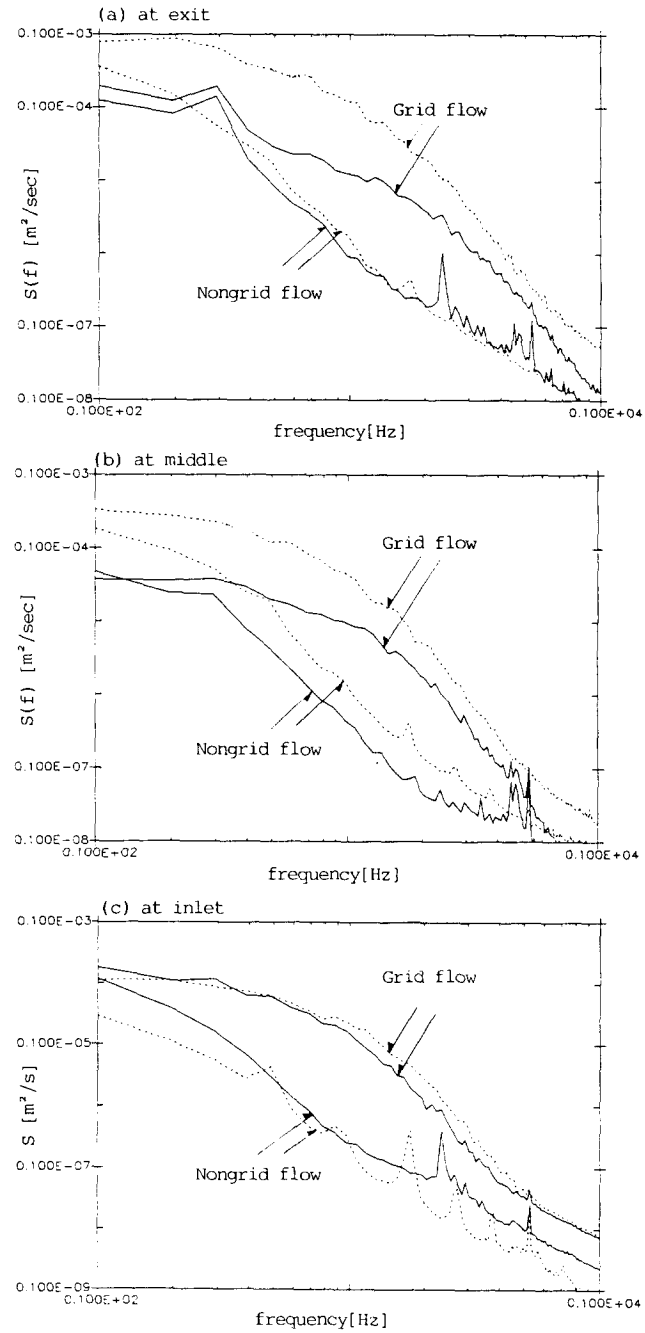

Fig. 6 Velocity spectra of grid flow and nongrid flow at (a)exit, (b)middle and (c)inlet of contraction[—— longitudinal turbulence and ·····lateral one]

the nongrid turbulence and S_o, a purified spectrum considered. The nongrid spectra can be considered to have flow contamination only which contain the consistent noises for every positions through contraction. Comparing with the grid spectra, the power were much lower than those of grid spectra but some of peaks were overshooted above the grid spectra. In the subtracted spectra the overshoots were disappeared and the spectra have the smooth shapes as follows[Figs. 7(a), (b), (c)]. Of course, there were the possibilities to have the thresholds by the subtraction at the frequency the special noises appeared so that the inverse trans-

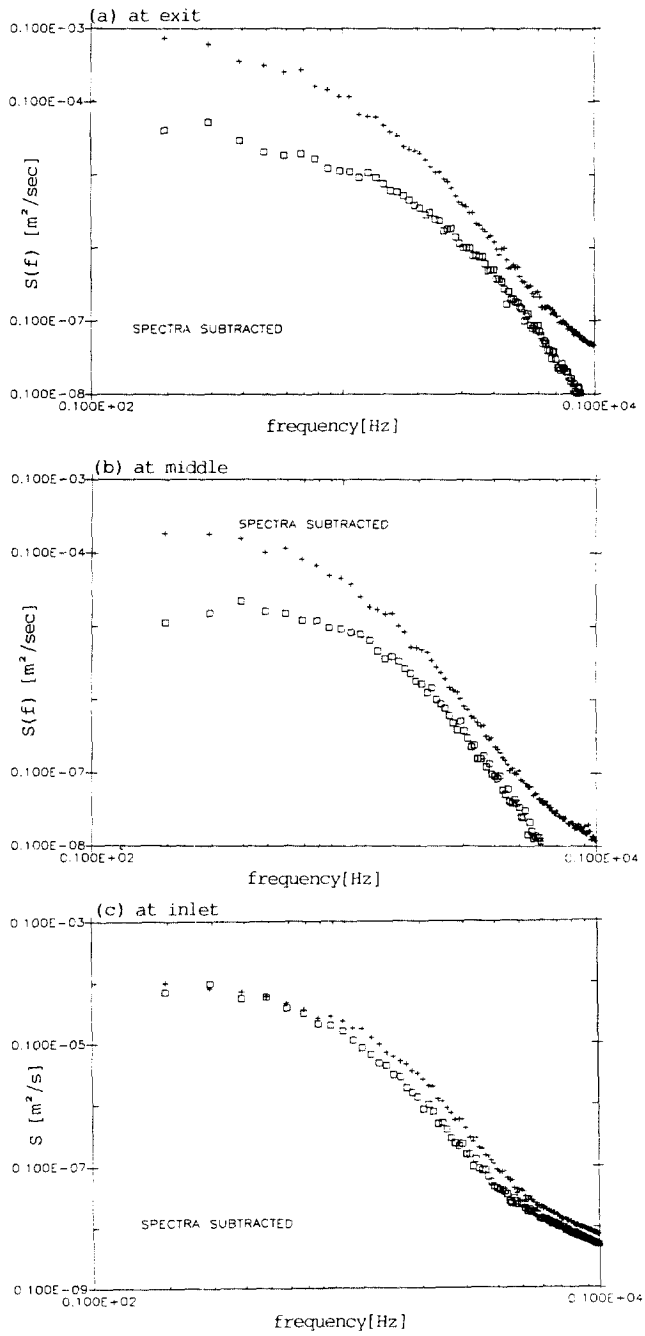

Fig. 7 Velocity spectra subrtacted at (a)exit, (b)middle and (c) inlet of contraction respectively. [□ □ □ □ □ □ longitudinal turbulence, + + + + + + lateral ones]

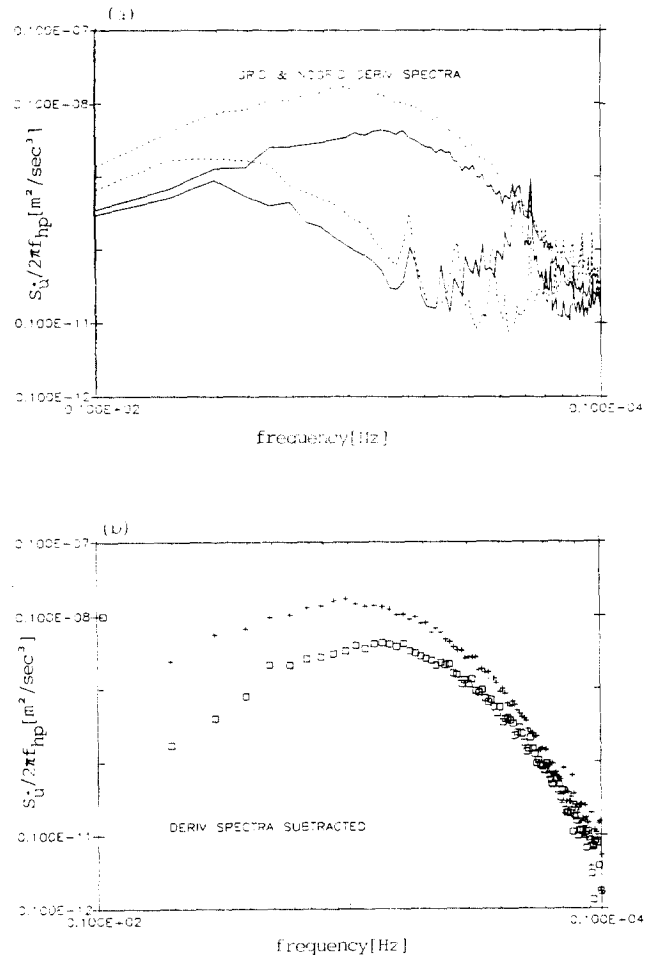

Fig. 8 (a) Derivative Spectra of Grid flow and Nongrid flow [□ □ □ □ □ □ : longitudinal component and + + + + + + + : lateral ones, the lower spectra are of nongrid parts], (b) subtracted results (where f_{hp} is 5kHz)

form of the subtracted spectra could be slightly less than the true values. But it was assured to be small enough after the comparison with the moment measurements.

From the linearity of the input signal ; $\dot{u}(t) = \dot{u}_x + \dot{u}_n$, the differential output $\dot{u}$ can be obtained by using the 1st order linear system, a simple electric differentiator, like as $\dot{e}_i = 2\pi f_{HP} e_o$, where $(\cdot)$ means the time derivative. Therefore, their spectra are also linear so that the subtraction technique can be applied as the same way in order to get the pure grid derivative spectra, i.e.,

$$S_{\dot{u}_g}(f) - S_{\dot{u}_{ng}}(f) = S_{\dot{u}_o}(f) \tag{10}$$

and $S_{\dot{u}}(f)$ is a spectrum of derivative signals as follow ;

$$S_{\dot{u}}(f) = \int_{-\infty}^{\infty} e^{j2\pi ft'} \overline{\dot{u}(t)\ \dot{u}(t+t')}\ dt' \tag{11}$$

and the figures are as follows [Figs. 8(a), (b)] ;

There is a mutual substitutional relation ship between the derivative and the velocity spectra such that

$$S_{\dot{u}}(f)/f^2 \sim S(f) \tag{12}$$

In high frequency range, the derivative spectra can be used as a good quality velocity spectra by use of the equation above because the derivative spectra has a distinct effect of the cutoff effect in high frequency range. On the contrary, the velocity spectra can be used to estimate a good quality derivative spectra in low frequency range by multiplying by f^2. By using this characteristics the combination of high frequency modification from the derivative spectra and the velocity spectra in low frequency can improve the final velocity spectrum. Therefore, the final form of spectrum can be used for calculating the moments by the inverse transforms(Fig. 9).

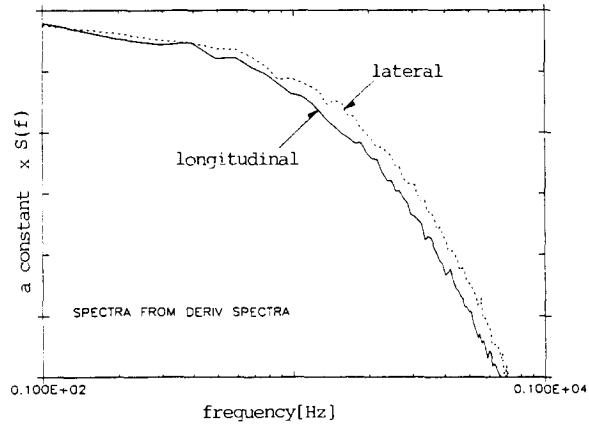

Fig. 9 Velocity spectra from derivative spectra using the relation(12) at contraction inlet

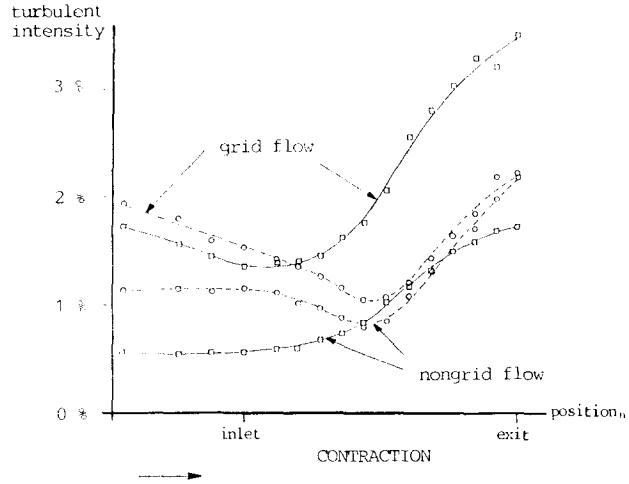

Fig. 10 Turbulence distributions along the contraction centerline [--O--O--longitudinal, --□--□--□ lateral and lower curves of each components are of nongrid cases]

4.3 Result of the Improvement

Following the procedures of the electrical noise reduction, the subtraction and the modification, the longitudinal turbulence was reduced about 1~1.5% roughly, near the contraction exit, which implies that the upstream contaminations have the critical effects to the downstream where the turbulence intensity is at best 5%, or less, while the lateral turbulence did not change so much as the longitudinal one(Fig. 10). The improved result reduces the amount of the production term substantially so that it can avoid the negative reading on the dissipation which is obtained from the difference between the mean convection and the production.

5. CONCLUSION

The moment and the spectra measurements supported the validity of the present subtraction hypothesis. Provided the proper statistical criterion from the coherent measurement which should be small enough, the subtraction hypothesis can be used as a powerful tool to get rid of the upstream flow contamination including the acoustic effects. The pure grid turbulence through the contraction can be obtained by the subtraction technique because the upstream contamination increases at the same rate as that of mean velocity through the contraction while the pure grid turbulence follows the vortex stretching mechanism. Therefore, the contraction turbulence must be reconsidered with the pure grid effect only.

REFERENCES

Champagne, F. H., Sleicher, C. A. and Wehmann, O. H., 1967, "Turbulence Measurements with Inclined Hot-wires, Part I. Heat Transfer Experiments with Inclined Hot-wire", JFM, Vol. 28. p. 153.

Comte-Bellot, G. and Corrsin, S., 1966, "The Use of a Contraction to Improve the Isotropy of Grid-generated Turbulence", JFM, Vol. 25, p. 657

Corrsin, S., 1963, Handbuch der physik, Ed. by Flugge, S. and Truesdell, C. A., Springer-Verlag, Berlin, Vol. VIII/2, p. 438.

Crow, S. C. and Champagne, F. H., 1971, "Orderly Structure in Jet Turbulence", JFM, Vol. 28, p.547.

Freymuth, P., 1968, "Noise in Hot-wire Anemometers", The Review of Scientific Instruments, Vol. 39, No. 4. p.550.

George, W. K., Beuther, P. D. and Lumley, J. L., 1978, "Processing of Random Signal", Proc. of Dynamic Flow Conf., Denmark.

George, W. K., Beuther, P. D. and Shabbir, A., 1987, "Polynomial Calibrations for Hot-wires in Thermally Varying Flows", ASME Symp. on Thermal Anemometry, Cincinnati, OH.

Han, Y. O., 1988, "The Effect of Contraction on Grid-generated Turbulence", Ph. D. Dissertation, State Univ. of New York at Buffalo.

Lumley, J. L. and Newman, G. R., 1977, "The Return to Isotropy of Homogeneous Turbulence", JFM, Vol. 82, p. 161.

Ramjee, V. and Hussain, A. K. M. F., 1976, "Influence of the Axisymmetric Contraction Ratio on Free-stream Turbulence", J. of Fluid Eng., Trans. ASME, p. 506.

Shabbir, A., 1983, "Investigation of the Functional Form of the Coefficients of the Reynolds-stress Closure", MS Thesis, State Univ. of New York at Buffalo.

Uberoi, M. S., 1956, "Effect of Wind-tunnel Contraction on Freestream Turbulence", J. of Aeronautical Sci., Aug., p. 754.